Code 186

DECLASSIFIED

[redacted]

UNCLASSIFIED

NRL REPORT NO. R-3173

X-BAND ANTENNA FOR AN/APQ-33(XB) JAM SYSTEM

★

DECLASSIFIED by NRL Contract
Declassification Team
Date: 19 DEC 2016
Reviewer's name:

Declassification authority: NAVY DECLASS GUIDE/NAVY DECLASS MANUAL, 11 DEC 2012, D8 SERIES

[redacted]

DISTRIBUTION STATEMENT A APPLIES.
Further distribution authorized by UNLIMITED only.

NAVAL RESEARCH LABORATORY

WASHINGTON, D.C.

DECLASSIFIED

DECLASSIFIED

[redacted]

[redacted]

NRL REPORT NO. R- 3

X-BAND ANTENNA FOR AN/APQ-33(XB) JAM SYSTE

K. W. Bewig

Approved by:

Mr. E. A. Speakman, Head, Radio Countermeasures Section
Dr. L. T. Bourland, Superintendent (Acting), Radio Division II

Problem No. 39R06-25 July 21, 1947

NAVAL RESEARCH LABORATOR

COMMODORE H. A. SCHADE, USN, DIRECTOR

WASHINGTON, D.C.

DECLASSIFIED

DECLASSIFIED [redacted]

[redacted]

DISTRIBUTION

BuShips	
Attn: Code 910B	10
Attn: Code 920	1
BuAer	
Attn: Code TD-4	1
CNO	
Attn: Code OP-413-B2	6
ONR	
Attn: Code N482	2
CO, ONR, Boston	1
Dir., USNEL	2
SNLO, USNELO, Ft. Monmouth	1
ANEESA	1
CG, AMC, Wright Field	
Attn: TSELO	1
CO, Watson Labs., AMC, Red Bank	
Attn: WLENG	1
CO, Watson Labs., AMC, Cambridge	1
CO, SCEL	1
CO, CSL	1
CO, ESL	1
Hdqts., USAF	
Attn: AC/AS-3, ACO	1
OCSigO	
Attn: SIGTM-S	1
RDB	
Attn: Library	2
Attn: Navy Secretary	1
Science and Technology Project	
Attn: Mr. J. H. Heald	2

DECLASSIFIED

CONTENTS

ABSTRACT

This report describes the development of an X-band antenna for use with the AN/APQ-33 (XB) Automatic Search and Jam System. (See Reference 1.) The antenna structure is designed to present zero drag for use on high speed airplanes. It radiates a circularly polarized wave having a pattern that will jam ground radars in all directions. The standing wave ratio is less than 1.27 over the frequency range of 8450 to 9350 megacycles.

A general design procedure is described for antennas of this type.

PROBLEM STATUS

Work on this problem is continuing. A series of antennas are being designed to cover wider frequency ranges (30 to 10,000 Mc).

X-BAND ANTENNA FOR AN/APQ-33(XB) JAM SYSTEM

INTRODUCTION

An antenna for an automatic search and jam system should have broad band characteristics, and it should be effective against any polarization of the radar signal. These requirements are best met for an airborne jammer against ground radars by an antenna which produces a circularly polarized wave having a pattern that radiates sufficient power within a cone drawn from the airplane to the horizon. It should be observed that the above antenna will not be effective against a radar that transmits a circularly polarized wave of the opposite direction sense. Dual antenna systems would be required to cover this case.

A solution to the problem has been obtained by placing a quarter-wave polarizing plate in a one inch circular guide (see Reference 2 and Appendix 1), and sealing the aperture of the guide with a dielectric button having a conical matching taper on its inner surface. Although the radiation pattern is not ideal in all planes of radiation, it is shown that the antenna will give protection against any ground radar in terms of reasonable jamming power compared to the reflected radar return from the airplane.

The ideal radiation pattern for this application is a sphere with the airplane located at its zenith. This pattern will give a constant ratio of jamming power to reflected power at any ground point. (See Reference 3, Reference 4, and Appendix 2.)

The half-power beam width through any cross section of a spherical pattern is 90 degrees. As the half-power beam widths obtained from unflared wave guides are less than 90 degrees, attempts were made to broaden these patterns by using concave dielectric lenses. (See Reference 5.) These lenses introduced considerable mismatch over broad frequency ranges, and attempts to adapt them to zero drag design were unsatisfactory.

The antenna presents a matched load in the measured frequency range from 8430 to 9350 megacycles for use with proposed magnetron power sources. Measurements have not been made to the extreme useful limits of operation due to the present lack of suitable measuring equipment. However, it is expected that similar antennas can be designed to center about any desired frequency from 3000 to 30,000 megacycles.

ANTENNA DESIGN

A circular horn was chosen in order to obtain symmetry of the radiation pattern to meet the requirement of complete azimuthal jamming coverage.

Reference 2 contains design curves for quarter-wave polarizing plates placed in rectangular or square wave guides. Circular guide plates can be designed from these curves by choosing a diameter having suitable cutoff frequencies for the TE_{11} and the TM_{01} circular guide modes. This diameter places the cutoff frequency for the TE_{11} mode at the low end of the desired operating range and the cutoff frequency for the TM_{01} mode at the high end of the range. The cutoff frequency for the TE_{11} mode is then taken as the cutoff frequency for the TE_{10} mode in a square guide. From this data the dimensions of the corresponding square guide can be determined, and Reference 2 can be used to design the quarter-wave polarizing plate. These dimensions are then used for the plate in the circular guide. This procedure has proven to be most satisfactory. Appendix 1 explains this method in detail.

Many types of dielectric lenses (see Reference 5) were tried in order to broaden the radiation patterns of the unflared circular guide to the required 90 degree half-power beam widths. All of these lenses had characteristic undesirable qualities. Narrow ranges of low standing wave ratios could be centered anywhere in the desired frequency range as a function of the lens spacing in front of the horn aperture, but no arrangement was found that gave low standing wave ratios over the entire frequency range. Although wide beam broadening could be obtained in some planes of polarization, in other planes the radiation pattern collapsed. Lenses placed in the aperture of the horn caused extremely high reflection. Attempts to obtain zero drag construction were also unsuccessful. These lenses were placed in wells so that their apertures were flush with a ground plane simulating the airplane airfoil. The horn was then mounted at an optimum distance behind the lens. All of these arrangements caused severe lobing of the radiation pattern, even in the forward direction, and again the pattern broadening collapsed in discrete planes of polarization. Figure 1 shows a typical set of radiation patterns taken in four planes of polarization for one of the lenses selected at random. In this case zero drag construction has not been attempted, and the beam lobing is not so severe.

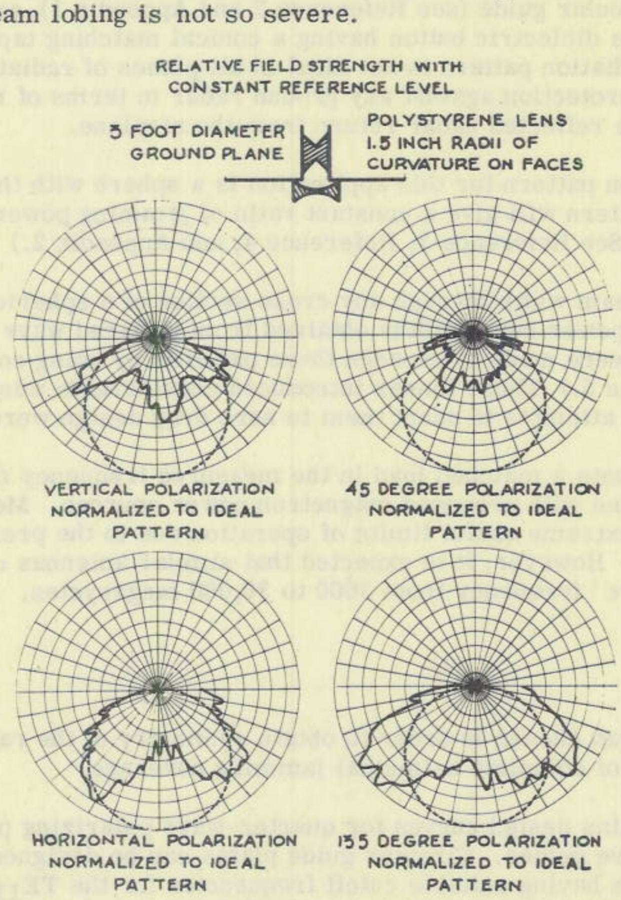

Fig. 1 - Radiation Patterns of a Typical Dielectric Lens Used with the Unflared Circular Wave Guide

Since a high degree of circularity and low values of standing wave ratios could be obtained from a quarter-wave plate in an open unflared wave guide, it was decided to investigate how closely this arrangement would approach the ideal spherical pattern. Zero drag construction could then be obtained by placing a flush dielectric button in the aperture of the guide, and matching could be provided by shaping the inner face of the button.

Figure 2 shows the final arrangement of the antenna based on this reasoning. The tapered dielectric button sealing the aperture of the horn has critical dimensions as shown by the standing wave ratios plotted on Figure 3.

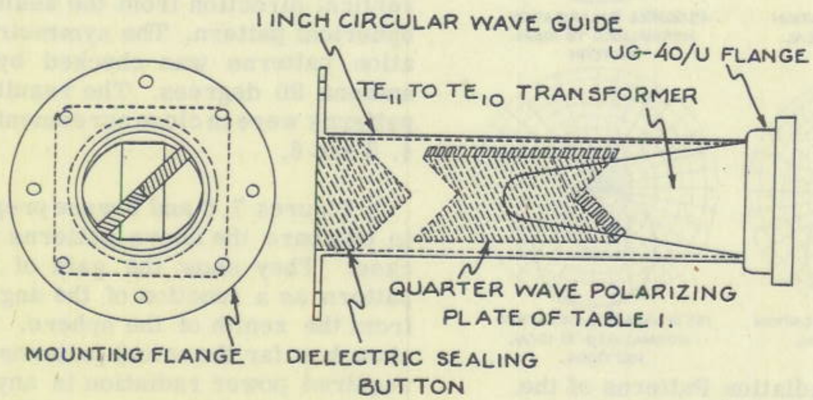

Fig. 2 - Mechanical Details of the X-Band Circularly Polarized Antenna (Laboratory Model)

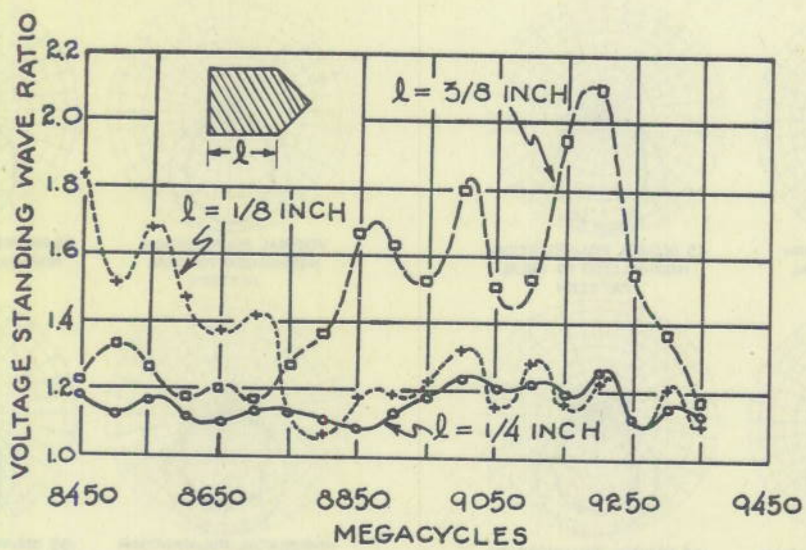

Fig. 3 - Standing Wave Ratios for Three Dielectric Buttons Used to Seal the X-Band Circularly Polarized Antenna (Laboratory Model)

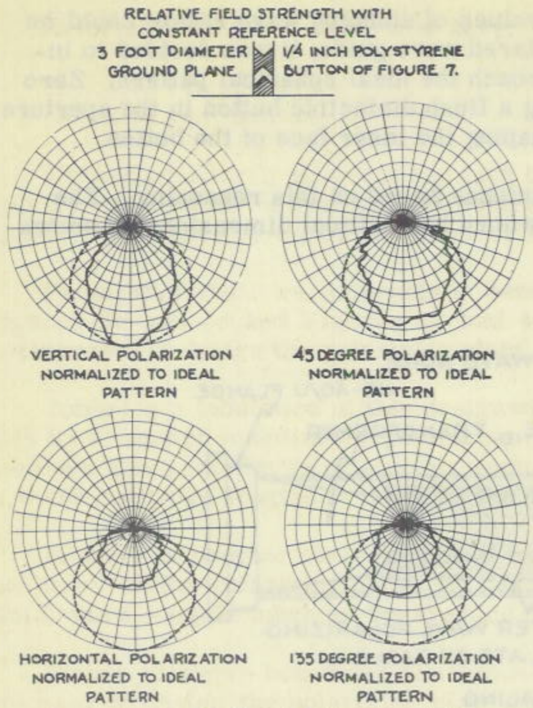

Fig. 4 - Radiation Patterns of the X-Band Circularly Polarized Antenna (Laboratory Model) 8600 Megacycles

The radiation patterns were measured in consecutive 22.5-degree planes of polarization. Four typical patterns for vertical, 45 degree, horizontal, and 135 degree polarization are displayed on Figures 4, 5 and 6. Each set of four patterns were taken over a five minute interval at constant power level with an automatic pattern plotter. Thus, these patterns simultaneously display the relative circularity between the four planes of polarization as well as the relative field strength referred to the vertical direction from the zenith of the ideal spherical pattern. The symmetry of the radiation patterns was checked by rotating the antenna 90 degrees. The resulting measured patterns were in close agreement with Figures 4, 5 and 6.

Figures 7, 8 and 9 were prepared in order to compare the above patterns with the ideal case. They show the gain of the spherical pattern as a function of the angles measured from the zenith of the sphere. These curves show how far the actual patterns fall below the required power radiation in any direction for complete jamming coverage. The original data

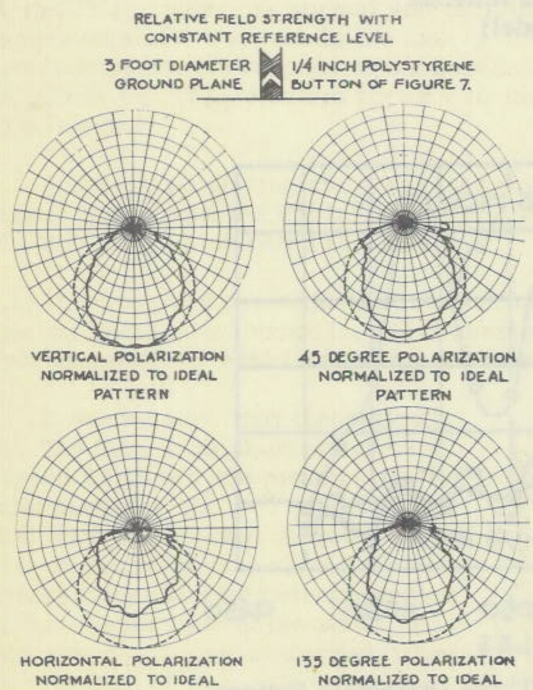

Fig. 5 - Radiation Patterns of the X-Band Circularly Polarized Antenna (Laboratory Model) 8950 Megacycles

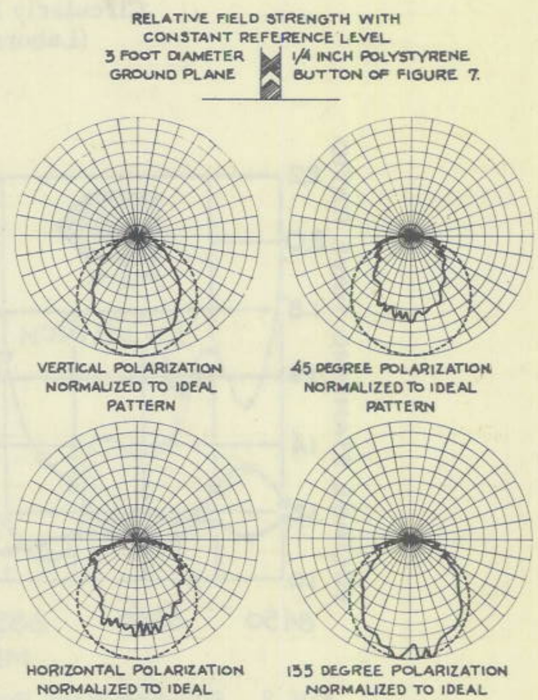

Fig. 6 - Radiation Patterns of the X-Band Circularly Polarized Antenna (Laboratory Model) 9350 Megacycles

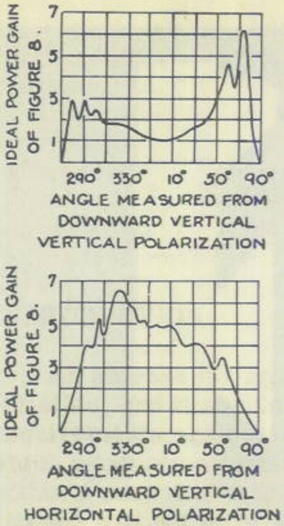

Fig. 7 - Power Gain of the Ideal Spherical Pattern from Figure 4

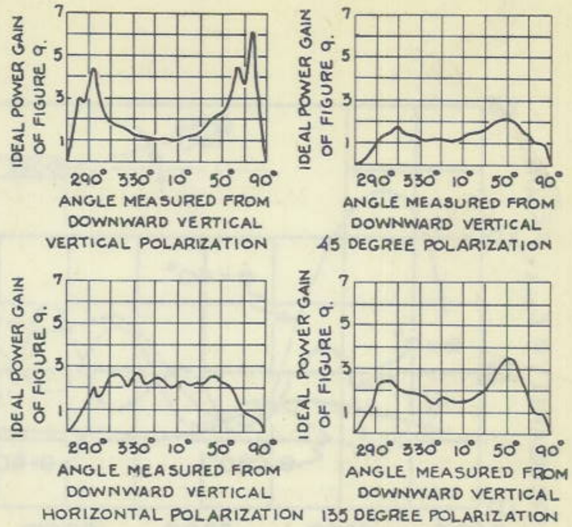

Fig. 8 - Power Gain of the Ideal Spherical Pattern from Figure 5

is normalized to the maximum radar cross section of the plane so that the most unfavorable conditions are covered. The absolute magnitude of the required jamming power contains a factor involving the characteristics of the ground radar and the characteristics of the noise power being radiated by the jamming airplane. The resulting figure for the most unfavorable direction is 6.5 times the ideal power. The calculations are based on an airplane in level flight with the antenna pointed vertically downward.

Figure 10 is an independent measurement of the circularity of the antenna over the entire frequency range. The values plotted here are not relative to the above selected planes of polarization, but they are the ratios of the maximum to the minimum response for all planes of polarization at each measured point. Circularities measured by rotating the antenna agree with Figure 10 as expected from the symmetry of the radiation patterns.

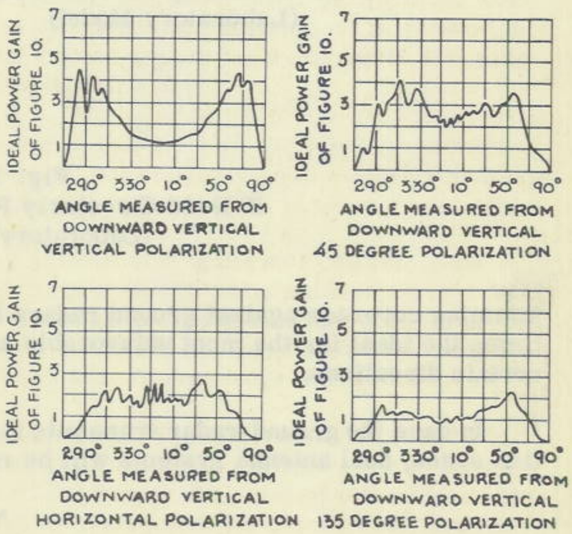

Fig. 9 - Power Gain of the Ideal Spherical Pattern from Figure 6

Figure 11 is a photograph of the laboratory model of the antenna.

CONCLUSIONS

This antenna provides a rugged, zero drag structure suitable for use on high speed airplanes. It radiates a circularly polarized wave having a pattern that will provide

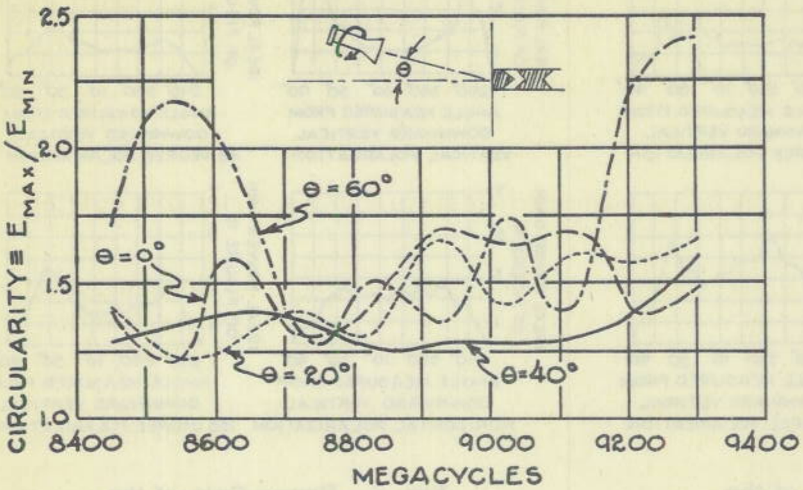

Fig. 10 - Circularity Measurements of the X-Band Circularly Polarized Antenna (Laboratory Model)

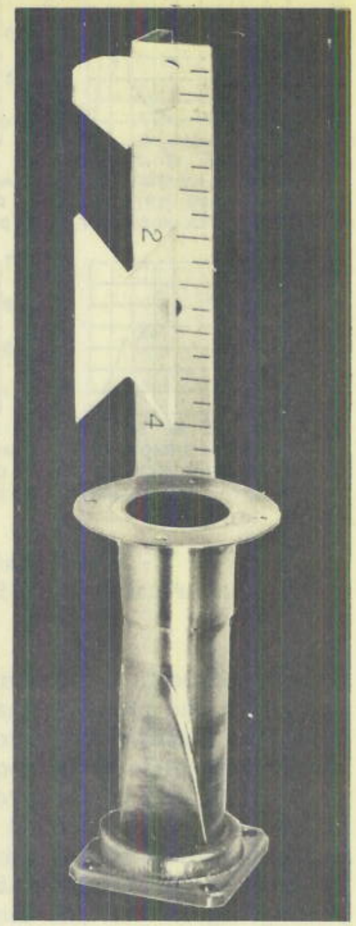

Fig. 11
X-Band Circularly Polarized Antenna
(Laboratory Model)

jamming coverage against ground radars in all directions. Powers of the order of 6.5 times the ideal for the most unfavorable aspect are required for complete screening in certain directions.

In case the ground radar transmits a circularly polarized wave of the opposite direction sense, dual antenna systems will be required for complete jamming coverage.

* * *

REFERENCES

1. BuShips Conf. ltr. ser. 08606 (913D-904) of 11 April 1946 to Director, NRL
2. RL Report no. 769, "Quarter-Wave Plate for Circular Polarization".
3. NRL file no. 2065, "Antennas for Radar Jammers".
4. RRL Report no. 411-298, "Review of Data on M2200 Fishhook Antennas".
5. RL Report no. 981, "X-Band Hemi-Isotropic Radiator".
6. "Reference Data for Radio Engineers," book, 1943, Federal Telephone and Radio Corporation.

Original data entered in NRL log books no.6752 and no. 6927

APPENDIX 1

This appendix describes a method of adapting Reference 2 to the design of a quarter-wave polarizing plate for a circular wave guide.

It should be pointed out that the proposed frequency range of 3000 to 30000 megacycles will require the use of 5 different sizes of wave guides. Standard sizes of wave guides should be adopted prior to the design of antennas to overlap this frequency range.

A one-inch circular guide was decided upon because it allowed for straightforward construction of the TE_{11} circular guide to TE_{10} square guide coupling transformer to a standard UG-40/U flange termination.

The useful range of operation of the one-inch diameter circular guide lies between the cutoff frequencies for the TE_{11} and the TM_{01} modes.

Given a one-inch diameter circular guide, we have the following relations (see Reference 6):

$$f_{c_{n,m}} = ck_{n,m}/2\pi = (3 \times 10^{10}/6.283)\, k_{n,m}$$

$$= .478 \times 10^{10} \times k_{n,m}$$

$$k_{n,m} = U_{n,m}/r \quad \text{or} \quad U'_{n,m}/r = U_{n,m}/1.27 \quad \text{or} \quad U'_{n,m}/1.27$$

where r is the radius of the wave guide in centimeters and U and U' is the root of the particular bessel function of interest (or its derivative), for TE and TM modes respectively.

$$f_c(TE_{11}) = .478 \times 10^{10} \times 1.841/1.27 = 6940 \text{ megacycles.}$$

$$f_c(TM_{01}) = .478 \times 10^{10} \times 2.405/1.27 = 9060 \text{ megacycles.}$$

These relations indicate that a smaller diameter wave guide would be desirable for the measured frequency range of 8400 to 9300 megacycles from the standpoint of mode suppression. Increased beam widths would be expected to result from the decreased aperture of the smaller wave guide. However, the above frequency range happened to be that of the available measuring equipment, and the one-inch diameter wave guide was chosen to facilitate the construction on the TE_{11} to TE_{10} mode coupling transformer as previously mentioned. No trouble has been experienced at 9300 megacycles from the TM_{01} mode of transmission. It was felt that the design principles of the antenna could be investigated with this unit, and the optimum dimensions of an overlapping series of similar units could then be designed to meet any frequency requirements.

We now equate $f_c(TE_{10})$ for the square guide to 6940 megacycles.

$$f_c(TE_{10}) = 6940 \text{ megacycles.}$$
$$\lambda_c(TE_{10}) = 4.32 \text{ centimeters.}$$

Referring to Figure 12 we now have:

2a = 4.32 centimeters
a = 2.16 centimeters.

We then arbitrarily choose a .150 inch thick Polystyrene strip as the quarter wave polarizing plate. This makes $\epsilon_2 = 2.55$ and $d/a = .1765$.

From this data we interpolate between Figures 3c and 3d and Figures 4c and 4d of Reference 5 to design the polarizing plate.

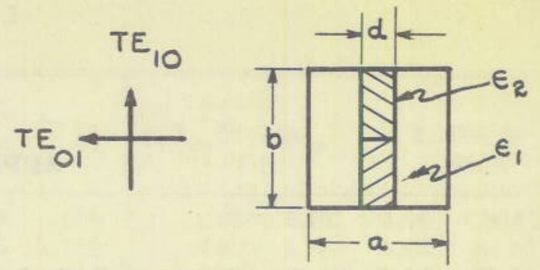

Fig. 12 - Cross Section of the Quarter Wave Polarizing Plate Placed in a Square Wave Guide

Table 1 is a tabulation of this design where L is the computed length of the polarizing plate to give a 90 degree phase shift between the assumed TE_{10} and the TE_{01} electric vectors in the square guide. The mean value, L_{mean}, of these computed lengths is taken as the design length of the polarizing plate.

In order to provide some degree of matching for the discontinuities introduced by the end faces of the polarizing plate, 90 degree notches are cut in the ends of the polarizing plate, and L_{mean} is taken as the average of the distances L_1 and L_2 of Figure 13.

Figure 13 shows how these dimensions are used to design the polarizing plate for the circular guide. This polarizing plate is oriented in the circular guide at 45 degrees to the direction of the main electric vector of the TE_{11} mode. Its normal and parallel components with respect to the axis of the polarizing plate correspond to the assumed TE_{10} and the TE_{01} electric vectors in the square guide.

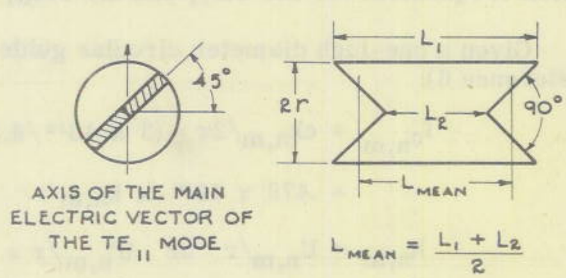

Fig. 13 - Dimensions of the Quarter Wave Polarizing Plate for the Circular Wave Guide Derived from the Computations for the Square Wave Guide Case

A similar polarizing plate was then designed by choosing d = .250 in. instead of .150 in. This data is tabulated in Table 2.

The computed phase shifts introduced between the TE_{10} and the TE_{01} components of the electric vectors for the two L_{mean} dimensions were then determined at each frequency. These figures are shown in the last column of Table 1 and Table 2, and the results are plotted in Figure 14.

It can be seen that theoretically the .250 inch thick plate is superior. Figure 15 shows the measured circularities for the two plates. The .250 inch thick plate is quite poor. This is probably caused by the relatively greater discontinuity presented by the thicker face of the plate. For this reason it was discarded from the design.

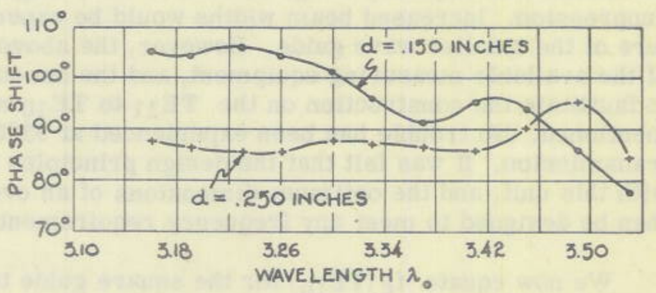

Fig. 14 - Computed Phase Shifts Introduced Between the TE_{10} and the TE_{01} Components of the Square Wave Guide Electric Vectors for 2 Different Polarizing Plates

Reference 2 is used in the following way to obtain the data for Table 1 and Table 2. (See Figures 12 and 13 for notation.)

The conditions for circularity, assuming equal TE_{10} and TE_{01} electric vectors in a rectangular or square wave guide, are given by the following relation:

$$L/\lambda_{10} - L/\lambda_{01} = 1/4 + n/2,$$
$$n = 0, 1, 2, 3, \ldots$$

$$L = (\lambda_{01} \times \lambda_{10})/4(\lambda_{01} - \lambda_{10})$$
when $n = 0$.

λ_{10} is determined from Figures 3a to 3e of Reference 2, depending upon the chosen values of d/a and ϵ_2.

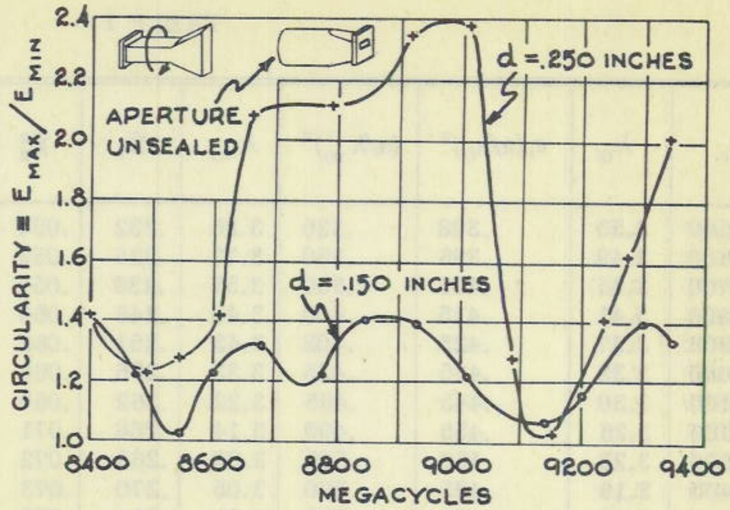

Fig. 15 - Measured Circularities of the Two Equivalent Circular Wave Guide Polarizing Plates Designed from the Data of Figure 3

λ_{01} is determined from the following relation:

$$(a/\lambda_{01})^2 = \epsilon_1 (a/\lambda_o)^2 + \bar{X}_2^2 - (a/2b)^2.$$

This equation is derived in Reference 2 in a rather complicated manner from the general transmission modes existing in a rectangular wave guide with a centered dielectric strip.

$\bar{X}_2$ is a parameter determined from Figures 4a to 4e of Reference 2, depending upon the chosen values of d/a and ϵ_2.

The tabulation of the data in Table 1 and Table 2 is then obtained in a straightforward manner.

* * *

TABLE 1

f_O	λ_O	$\epsilon_1 (a/\lambda_O)^2$	$(a/\lambda_{10})^2$	λ_{10}	$\overline{X}_2$	$\overline{X}_2^2$	$(a/\lambda_{01})^2$	λ_{01}	L	Phase Shift
8500	3.53	.388	.325	3.85	.232	.054	.192	5.01	4.16	78.4°
8600	3.49	.396	.350	3.72	.235	.055	.201	4.91	3.84	86.1°
8700	3.45	.405	.380	3.57	.239	.057	.212	4.79	3.50	94.3°
8800	3.41	.415	.400	3.48	.245	.060	.225	4.64	3.48	95.0°
8900	3.37	.425	.408	3.43	.251	.063	.238	4.50	3.61	91.5°
9000	3.33	.435	.435	3.33	.255	.065	.250	4.39	3.45	95.8°
9100	3.30	.443	.465	3.22	.262	.069	.262	4.29	3.22	102.5°
9200	3.26	.455	.490	3.14	.266	.071	.276	4.18	3.16	104.5°
9300	3.23	.463	.505	3.09	.268	.072	.285	4.12	3.09	107.0°
9400	3.19	.425	.520	3.05	.270	.073	.298	4.02	3.16	104.5°
9500	3.16	.484	.535	3.01	.273	.075	.309	3.96	3.14	105.0°

d = .150 inch, d/a = .1765, ϵ_2 = 2.55.

$$L_{mean} = \frac{4.16 + 3.09}{2} = 3.63 \text{ centimeters.}$$

TABLE 2

f_O	λ_O	$\epsilon_1 (a/\lambda_O)^2$	$(a/\lambda_{10})^2$	λ_{10}	$\overline{X}_2$	$\overline{X}_2^2$	$(a/\lambda_{01})^2$	λ_{01}	L	Phase Shift
8500	3.53	.388	.500	3.10	.347	.121	.259	4.33	2.72	84.8°
8600	3.49	.396	.525	3.03	.354	.125	.271	4.22	2.41	95.7°
8700	3.45	.405	.542	2.98	.360	.130	.285	4.11	2.56	90.0°
8800	3.41	.415	.565	2.92	.364	.133	.298	4.02	2.67	86.4°
8900	3.37	.425	.585	2.97	.370	.137	.312	3.93	2.66	86.8°
9000	3.33	.435	.605	2.82	.376	.142	.327	3.84	2.65	87.2°
9100	3.30	.443	.625	2.78	.382	.146	.339	3.77	2.65	87.2°
9200	3.26	.455	.640	2.74	.390	.152	.357	3.67	2.70	85.4°
9300	3.23	.463	.660	2.70	.395	.156	.369	3.61	2.68	86.3°
9400	3.19	.475	.680	2.66	.400	.160	.385	3.54	2.68	86.3°
9500	3.16	.484	.710	2.61	.405	.164	.398	3.48	2.61	88.5°

d = .250 inch, d/a = .289, ϵ_2 = 2.55.

$$L_{mean} = \frac{2.72 + 2.41}{2} = 2.57 \text{ centimeters.}$$

APPENDIX 2

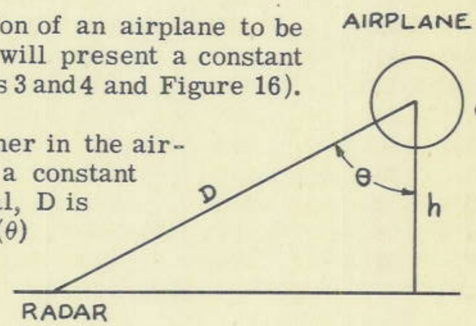

Fig. 16 - Notation for the Relations Derived in Appendix 2

If we assume the maximum radar cross section of an airplane to be drawn as an equivalent sphere, then the airplane will present a constant target to a ground radar in any aspect (see References 3 and 4 and Figure 16).

The field strength at the radar due to a jammer in the airplane is given by $F_1 = (k_1/D) \times f(\theta)$ where k_1 is a constant involving the characteristics of the jamming signal, D is the slant range from the airplane to the radar, and $f(\theta)$ is a function of the radiation pattern of the jamming signal.

The reflected field strength from the airplane of the transmitted radar signal is given by $F_2 = (k_2/D^2) \times \sigma$ where k_2 is a constant involving the characteristics of the radar system, D is again the slant range from the airplane to the radar, and σ is the radar cross section of the airplane.

For a constant field strength ratio of jamming signal to radar return we equate these two relations:

$$(k_1/D) \times f(\theta) = (k_2/D^2) \times \sigma$$
$$f(\theta) = (k_2/k_1)(\sigma/D) = k/D$$

where k is now a constant involving the characteristics of both the radar system and the jamming system (including the maximum radar cross section of the airplane). This constant can be written in terms of the absolute magnitude of the jamming power required to effectively jam the ground radar.

The slant range $D = h/\cos\theta$.
And $f(\theta) = (k/h) \times \cos\theta$

where h is the height of the airplane.

Thus, we see that for an airplane in level flight, the radiation pattern required to give a constant ratio of jamming field strength to radar return is proportional to $\cos\theta$, where θ is the angle measured from the downward vertical drawn from the airplane. The shape of this pattern is a circle. It becomes a sphere for complete azimuthal coverage.

* * *

PRNC-3687-11-20-47-500